A DISCRETE-TIME WAVELET TRANSFORM BASED ON A CONTINUOUS DILATION FRAMEWORK

Wei Zhao and Raghuveer M. Rao

Center for Imaging Science/
Electrical Engineering Department
Rochester Institute of Technology
79 Lomb Memorial Drive
Rochester, NY 14623-5603
Tel: (716)475-2185
Email: wxz1756@cis.rit.edu

ABSTRACT

In this paper we present a new form of wavelet transform. Unlike the continuous wavelet transform (CWT) or discrete wavelet transform (DWT), the mother wavelet is chosen to be a discrete-time signal and wavelet coefficients are computed by correlating a given discrete-time signal with continuous dilations of the mother wavelet. The results developed are based on the definition of a discrete-time scaling (dilation) operator through a mapping between the discrete and continuous frequencies. The forward and inverse wavelet transforms are formulated. The admissibility condition is derived, and examples of discrete-time wavelet construction are provided. The new form of wavelet transform is naturally suited for discrete-time signals and provides analysis and synthesis of such signals over a continuous range of scaling factors.

1. INTRODUCTION

The conventional discrete wavelet transform (DWT) [1, 2, 5, 6] provides a formulation over a dyadic set of scaling factors. However, in some wavelet applications, information at scaling factors other than those values on the dyadic grid is required. The conventional continuous wavelet transform (CWT) [2] provides information at scaling factors over a continuum. But, as the CWT is generally computed by using the samples of continuous-time wavelets, the computational complexity increases with the scaling factor. In both DWT and CWT, the set of wavelets are continuous-time signals. However, if the signal to be analyzed is inherently discrete-time, it is natural to choose a discrete-time signal as the mother wavelet and provide analysis and synthesis based on a set of wavelets which are discrete-time. In this paper we present a new formulation of wavelet transform in which the wavelets are all discrete-time signals, and continuous dilations of the mother wavelet are used to form a discrete-time wavelet transform over continuous scaling factors.

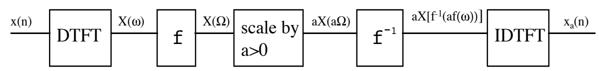

Figure 1: Block diagram of the discrete-time, continuous-dilation scaling operator. (I)DTFT: (inverse) discrete-time Fourier transform; f: frequency warping transform.

2. DISCRETE-TIME SCALING OPERATOR

Generally the scaling or dilation operation of a discrete signal $x(n)$ by an arbitrary factor is not well defined. It is difficult to obtain an interpretation of scaling in the discrete-time domain that is as unambiguous as that in the continuous-time domain. We present here a new approach for discrete-time scaling that can handle continuous scaling factors. We define the discrete-time scaling operator in a way that effectively amounts to converting $x(n)$ into a continuous-time signal through an invertible transform, applying the scaling operation to the continuous-time signal and finally mapping the signal back to the discrete-time domain. The definition is actually based on a warping transform in the frequency domain (Figure 1).

Definition 1 *A function $f(\ )$ is a discrete-time frequency (ω) to continuous-time frequency (Ω) warping transform if and only if:*

1. *In $\Omega = f(\omega)$, $\omega \in [-\pi, \pi]$ and Ω is the real line.*
2. *The transform is one-to-one.*

3. *$f(\,)$ is anti-symmetric about the origin, i.e. $f(-\omega) = -f(\omega)$. Furthermore, it is differentiable and monotonic in $[-\pi, \pi]$.*

4. *$f(0) = 0$.*

The defined discrete-time scaling operator gives the following input-output relationship in the frequency domain,

$$Y(\omega) = aX[\Lambda_a(\omega)], \tag{1}$$

where $X(\omega)$ and $Y(\omega)$ are discrete-time Fourier transforms of the input and output sequences, respectively, and

$$\Lambda_a(\omega) = f^{-1}[af(\omega)]. \tag{2}$$

3. DISCRETE-TIME CONTINUOUS-DILATION WAVELET TRANSFORMS

3.1. The Forward and Inverse Transforms

Let $\psi(n)$ be a discrete-time sequence and $\Psi(\omega)$ be its discrete-time Fourier transform defined by

$$\Psi(\omega) = \mathcal{G}[\psi(n)] = \sum_n \psi(n) e^{-j\omega n}, \tag{3}$$

where $\mathcal{G}$ denotes the discrete-time Fourier transform. Let

$$\Psi_a(\omega) = \sqrt{\Lambda_a'(\omega)}\,\Psi[\Lambda_a(\omega)], \tag{4}$$

where $'$ denotes the first derivative with respect to ω. Let

$$\psi_a(n) = \mathcal{G}^{-1}[\Psi_a(\omega)], \tag{5}$$

where $\mathcal{G}^{-1}$ is the inverse discrete-time Fourier transform. The discrete-time continuous-dilation wavelet transform (DCWT) is defined by choosing $\psi(n)$ as the mother wavelet and $\psi_a(n)$ as the wavelet at scale level a. It can be shown that $\psi(n)$ and $\psi_a(n)$ have the same energy. For a discrete-time sequence $x(n)$ and mother wavelet $\psi(n)$, the wavelet transform coefficients, $W_\psi(a, n)$, are computed as the inner products of $x(n)$ and translations of $\psi_a(n)$.

$$W_\psi(a, n) = \langle x(m), \psi_a(m - n)\rangle, \tag{6}$$

where $\langle\,\rangle$ denotes the inner product. The frequency domain representation of the forward DCWT is given by

$$W_\psi(a, n) = \frac{1}{2\pi}\int_{-\pi}^{\pi} X(\omega)\sqrt{\Lambda_a'(\omega)}\,\Psi^*[\Lambda_a(\omega)]e^{j\omega n}d\omega, \tag{7}$$

where $X(\omega)$ and $\Psi(\omega)$ are the discrete-time Fourier transforms of $x(n)$ and $\psi(n)$, and * denotes the complex conjugate. The inverse discrete-time continuous-dilation wavelet transform (IDCWT) is given by

$$\hat{x}(n) = \frac{1}{C_\psi}\int_0^\infty \langle W_\psi(a, m), \hat{\psi}_a^*(m - n)\rangle da, \tag{8}$$

where

$$C_\psi = \int_{-\pi}^{\pi} f(\alpha)|\Psi(\alpha)|^2 d\alpha, \tag{9}$$

and

$$\hat{\psi}_a(n) = \mathcal{G}^{-1}\left[\frac{[f(\omega)]^2\sqrt{\Lambda_a'(\omega)}\,\Psi^*[\Lambda_a(\omega)]}{f'(\omega)}\right] \tag{10}$$

is the IDCWT wavelet at scale a. Note that different mother wavelets are used for the forward and inverse transforms. The relationship between the frequency spectrum, $\Psi(\omega)$, of the DCWT mother wavelet $\psi(n)$, and the frequency spectrum, $\hat{\Psi}(\omega)$, of the IDCWT mother wavelet $\hat{\psi}(n)$, is

$$\hat{\Psi}(\omega) = \frac{[f(\omega)]^2}{f'(\omega)}\Psi(\omega). \tag{11}$$

The admissibility condition [1] of the DCWT is

$$C_\psi = \int_{-\pi}^{\pi} f(\alpha)|\Psi(\alpha)|^2 d\alpha < \infty. \tag{12}$$

It is generally required that the frequency spectrum $\Psi(\omega)$ of the mother wavelet satisfies $\Psi(\pm\pi) = 0$. However, there is no restriction on the value of $\Psi(0)$.

3.2. Bilinear Transform Based DCWT and IDCWT

We discuss the DCWT and IDCWT for the case of bilinear transform [4] in which

$$f(\omega) = 2\tan(\omega/2). \tag{13}$$

For simplicity, we will only discuss constructions of real-valued, bandlimited wavelets and their corresponding DCWT and IDCWT. Let $\psi(n)$ be a discrete-time signal and $\Psi(\omega)$ be its discrete-time Fourier transform which satisfies

1. $|\Psi(\omega)| < \infty$ for all $\omega \in [-\pi, \pi]$.
2. $\Psi(\omega)$ is symmetric about the origin.
3. Bandlimitedness. $\Psi(\omega) = 0$ for $\omega \in [0, \omega_1]$ and $\omega \in [\omega_2, \pi]$, where $0 \le \omega_1 < \omega_2 \le \pi$.

It is easy to verify that $\psi(n)$ satisfies the admissibility condition and thus is a valid DCWT mother wavelet. The DCWT wavelet at scale a, $\psi_a(n)$, will then have a frequency spectrum

$$\Psi_a(\omega) = \sqrt{\Lambda_a'(\omega)}\,\Psi[\Lambda_a(\omega)]. \tag{14}$$

$\psi_a(n)$ is also bandlimited and the two ends of the pass band are given by

$$\omega_1' = 2\tan^{-1}[\tan(\omega_1/2)/a] \text{ and } \omega_2' = 2\tan^{-1}[\tan(\omega_2/2)/a]. \tag{15}$$

If $0 < a < 1$, then $\omega_1' \ge \omega_1$ and $\omega_2' \ge \omega_2$, the whole pass band shifts to the right. If $a > 1$, then the whole pass band shifts to the left. Along with the shifting of the whole pass band in one direction, the bandwidth of the pass band also changes. Let $\Delta\omega$ and $\Delta\omega'$ be the bandwidths of the mother wavelet $\phi(n)$ and the wavelet $\phi_a(n)$. It is found that

- If $0 < a < 1$, then

$$\begin{cases} \Delta\omega' > \Delta\omega & \text{if } \tan(\omega_1/2)\tan(\omega_2/2) < a \\ \Delta\omega' = \Delta\omega & \text{if } \tan(\omega_1/2)\tan(\omega_2/2) = a \\ \Delta\omega' < \Delta\omega & \text{otherwise} \end{cases}$$

- If $a > 1$ then

$$\begin{cases} \Delta\omega' > \Delta\omega & \text{if } \tan(\omega_1/2)\tan(\omega_2/2) > a \\ \Delta\omega' = \Delta\omega & \text{if } \tan(\omega_1/2)\tan(\omega_2/2) = a \\ \Delta\omega' < \Delta\omega & \text{otherwise} \end{cases}$$

In the first example of the next section, $\omega_1 = 0$ and $\omega_2 = \pi/2$. As a changes, ω_1 remains at the origin, while ω_2 shifts to the right if $0 < a < 1$ and shifts to the left if $a > 1$. This gives a dilated frequency spectrum and thus a compressed wavelet when $0 < a < 1$, and a dilated wavelet when $a > 1$. In the second example, $\omega_1 = \pi/4$ and $\omega_2 = 3\pi/4$. Note that $\tan(\omega_1/2)\tan(\omega_2/2) = 1$. It is found that $\Delta\omega' < \Delta\omega$ for both $0 < a < 1$ and $a > 1$. Therefore, if $0 < a < 1$, both ω_1 and ω_2 shift to the right and the bandwidth decreases; if $a > 1$, both ω_1 and ω_2 shift to the left and the bandwidth still decreases. This eventually results in a compressed wavelet when $0 < a < 1$ and a dilated wavelet when $a > 1$.

Example 1: $\omega_1 = 0, \omega_2 = \pi/2$

Consider a discrete-time DCWT mother wavelet $\psi(n)$ which has the following frequency spectrum in $[-\pi, \pi]$

$$\Psi(\omega) = \begin{cases} |\sin(2\omega)| & \text{if } |\omega| \in [0, \pi/2] \\ 0 & \text{otherwise} \end{cases} \tag{16}$$

The spectrum $\Psi_a(\omega)$ of the DCWT wavelet at scale a is

$$\Psi_a(\omega) = \begin{cases} \left| \frac{2a\sqrt{a}\sin(\omega)[\cos^2(\omega/2)-a^2\sin^2(\omega/2)]}{[\cos^2(\omega/2)+a^2\sin^2(\omega/2)]^{5/2}} \right| \\ \qquad\qquad \text{if } |\omega| \in [0, 2\tan^{-1}(\frac{1}{\sqrt{2}a})] \\ 0 \qquad\qquad \text{otherwise} \end{cases} \tag{17}$$

The spectrum $\hat{\Psi}_a(\omega)$ of the IDCWT wavelet at scale a is

$$\hat{\Psi}_a(\omega) = \begin{cases} \left| \frac{8a\sqrt{a}\sin^2(\omega/2)\sin(\omega)[\cos^2(\omega/2)-a^2\sin^2(\omega/2)]}{[\cos^2(\omega/2)+a^2\sin^2(\omega/2)]^{5/2}} \right| \\ \qquad\qquad \text{if } |\omega| \in [0, 2\tan^{-1}(\frac{1}{\sqrt{2}a})] \\ 0 \qquad\qquad \text{otherwise} \end{cases} \tag{18}$$

Figure 2 shows the example DCWT mother wavelet and DCWT wavelets at different scales. Figure (3) shows the example IDCWT mother wavelet and IDCWT wavelets at

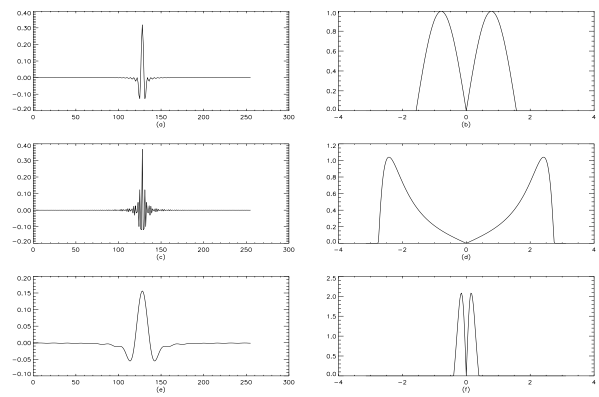

Figure 2: Example of DCWT bandlimited wavelet for the bilinear case. The pass band is located between $\omega = 0$ and $\omega = \pi/2$. (a) the DCWT mother wavelet; (c) DCWT wavelet at scale $a = 0.2$; (e) DCWT wavelet at $a = 5$; (b) (d) (f) frequency spectra of (a) (c) (e) respectively.

different scales. The IDCWT constant in this case is $C_\psi = 4/3$. Figure 4 shows the scalogram of the DCWT of a chirp function [3]

$$x(n) = \sin[\pi n^2/(2N)], \text{ for } n = 0, 1, ..., N \tag{19}$$

using this wavelet. The continuous changing of the frequency is apparent.

Example 2: $\omega_1 = \pi/4, \omega_2 = 3\pi/4$

The frequency spectrum of the DCWT mother wavelet in this example is given by

$$\Psi(\omega) = \begin{cases} |\cos(2\omega)| & \text{if } |\omega| \in [\pi/4, 3\pi/4] \\ 0 & \text{otherwise} \end{cases} \tag{20}$$

The DCWT wavelet at scale a has the following spectrum.

$$\Psi_a(\omega) = \begin{cases} \left| \frac{\sqrt{a}[\cos^4(\omega/2)+a^4\sin^4(\omega/2)-3/2\sin^2(\omega)]}{[\cos^2(\omega/2)+a^2\sin^2(\omega/2)]^{5/2}} \right| \\ \qquad\qquad \text{if } |\omega| \in [2\tan^{-1}(\frac{\pi}{8}), 2\tan^{-1}(\frac{3\pi}{8})] \\ 0 \qquad\qquad \text{otherwise} \end{cases} \tag{21}$$

The frequency spectrum of the IDCWT wavelet at scale a is given by

$$\Psi_a(\omega) = \begin{cases} \left| \frac{4\sqrt{a}\sin^2(\omega)[\cos^4(\omega/2)+a^4\sin^4(\omega/2)-3/2\sin^2(\omega)]}{[\cos^2(\omega/2)+a^2\sin^2(\omega/2)]^{5/2}} \right| \\ \qquad\qquad \text{if } |\omega| \in [2\tan^{-1}(\frac{\pi}{8}), 2\tan^{-1}(\frac{3\pi}{8})] \\ 0 \qquad\qquad \text{otherwise} \end{cases} \tag{22}$$

The IDCWT constant is $C_\psi = 0.558$. Figure 5 and 6 show plots of these DCWT and IDCWT wavelets at different scales. By changing the value of a and correlating the wavelet thus obtained with a given signal, different regions of the frequency spectrum of the given function are covered by the DCWT.

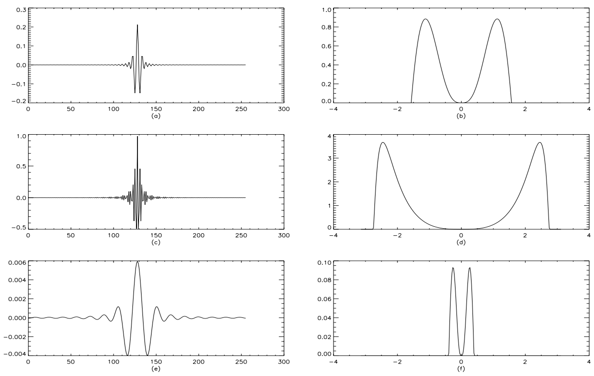

Figure 3: Example of IDCWT bandlimited wavelet for the bilinear case. The pass band is located between $\omega = 0$ and $\omega = \pi/2$. (a) the IDCWT mother wavelet; (c) IDCWT wavelet at scale $a = 0.2$; (e) IDCWT wavelet at $a = 5$; (b) (d) (f) frequency spectra of (a) (c) (e) respectively.

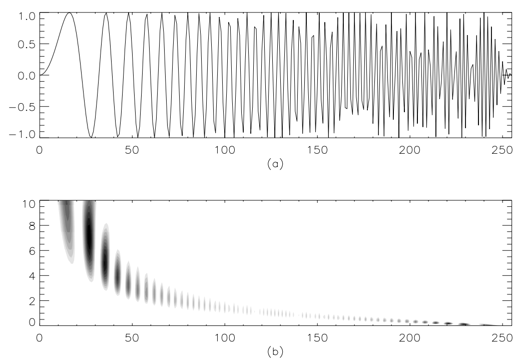

Figure 4: DCWT of a chirp function. (a) input; (b) scalogram of the DCWT.

4. CONCLUSION

The DCWT and IDCWT framework presented in this paper offers advantages in that it uses a set of discrete-time wavelets and is able to accommodate continuous dilations of the mother wavelet to provide analysis and synthesis of a discrete-time signal. It provides a potential tool for applications such as pattern recognition, image processing, etc., that require information of dilations of a discrete signal at arbitrary scaling factors.

5. REFERENCES

[1] I. Daubechies. Orthonormal bases of compactly supported wavelet. *Commun. Pure Appl. Math.*, 41:909–996, Nov. 1988.

[2] I. Daubechies. *Ten Lectures on Wavelets*. SIAM, 1992.

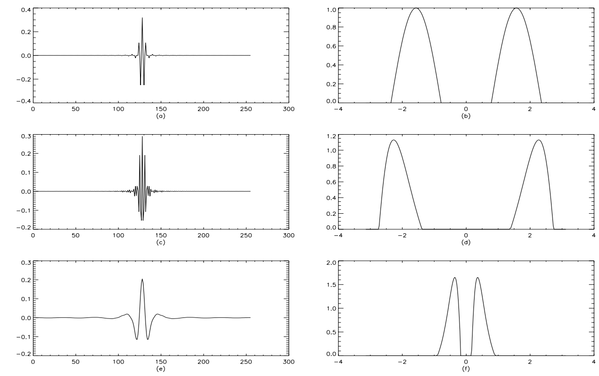

Figure 5: Example of DCWT bandlimited wavelet for the bilinear case. The pass band is located between $\omega = \pi/4$ and $\omega = 3\pi/4$. (a) the DCWT mother wavelet; (c) DCWT wavelet at scale $a = 0.5$; (e) DCWT wavelet at $a = 5$; (b) (d) (f) frequency spectra of (a) (c) (e), respectively;

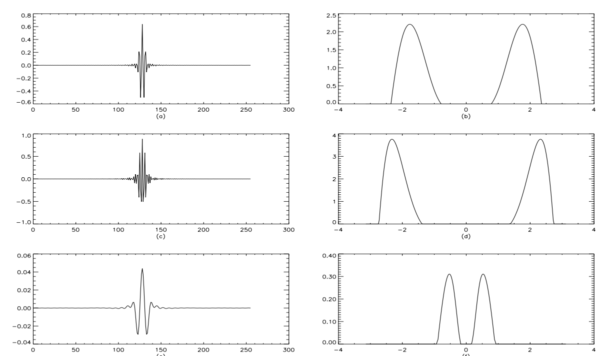

Figure 6: Example of IDCWT bandlimited wavelet for the bilinear case. The pass band is located between $\omega = \pi/4$ and $\omega = 3\pi/4$. (a) the IDCWT mother wavelet; (c) IDCWT wavelet at scale $a = 0.5$; (e) IDCWT wavelet at $a = 5$; (b) (d) (f) frequency spectra of (a) (c) (e) respectively;

[3] D. J. Gaskill. *Linear Systems, Fourier Transforms, and Optics*. John Wiley & Sons, 1978.

[4] A. D. Poularikas and S. Seely. *Signals and Systems*. PWS-KENT, Boton, 1991.

[5] M. J. Shensa. The discrete wavelet transform: Wedding the a trous and mallat algorithms. *IEEE Trans. on Signal Processing*, 40(10):2464–2482, Oct. 1992.

[6] G. Strang. Wavelets and dilation equations: A brief introduction. *SIAM Review*, 31:614–627, Dec. 1989.